Electric Power Systems Research 210 (2022) 108068

Contents lists available at ScienceDirect

Electric Power Systems Research

journal homepage: www.elsevier.com/locate/epsr

Full-length article

Optimal subtransmission switching using a reliability simulation-based multi-objective optimization model

Zambrano-Asanza Sergio [a,b,*], Proano Barros Tatiana [c], Banegas Dutan Stalin [c], Lema Guaman Edwin [b], Franco John Fredy [a,d]

[a] Department of Electrical Engineering, São Paulo State University – UNESP, Ilha Solteira, SP, Brazil
[b] Department of Planning, CENTROSUR Electric Distribution Utility, Cuenca, Ecuador
[c] School of Electrical Engineering, University of Cuenca, Cuenca, Ecuador
[d] School of Energy Engineering, São Paulo State University – UNESP, Rosana, Brazil

ARTICLE INFO

Keywords:
Distribution planning
NSGA-II, optimal switching
reliability
subtransmission system

ABSTRACT

The growth of subtransmission network aims at satisfying load growth, maintaining a contingency level, and providing a high quality and reliable electricity service. Utilities direct the investments to reinforce this system and thus a meshed network with multiple-point feeding to the transmission system arises. At this point, an efficient alternative to achieve these objectives is to carry out a diagnosis of the network architecture and, taking advantage of the switching capability, to plan the switching of the subtransmission lines. An optimal subtransmission switching approach is proposed based on constrained multi-objective optimization that deals with energy losses and reliability, in addition to using information on the characteristics of loads and generation. A simulation-based optimization framework is constructed using the non-dominated genetic classification algorithm NSGA-II in the optimization phase and reliability assessment during simulation phase. As a result, a set of non-dominated solutions approximating the Pareto front is obtained, which allows the planner to make decisions based on its priorities and needs. The performance of the proposal is assessed with a real subtransmission system of an Ecuadorian power utility. This approach to the operational planning of a meshed subtransmission network constitutes a powerful decision-making tool that could be adopted by distribution utilities.

1. Introduction

The subtransmission system constitutes an intermediary between the transmission power supply and the primary medium-voltage distribution network [1]. The most common voltage levels are 69, 115, and 138 kV [2], and their extension depends on the geographic reality of each electric utility. There could be more than one feeding point from the transmission network and the simultaneous operation is known as multiple-point feeding [3].

The expansion of the subtransmission network should first meet the load growth and then provide greater quality and reliability of the energy supply. In this way, the need for a meshed network emerges to have one or more additional feeding point, thus guaranteeing the service availability [3]. The planning of a subtransmission network is influenced by reserve capacity and a specific contingency level (e.g., N-1 or N-2 criteria). As a result of this contingency-based planning, there can be two transformers per substation and the network becomes a meshed grid [2]. Other than reliability enhancement, such meshed operation can bring additional benefits such as better voltage control [3].

The planning cycle described previously is also influenced by changes in consumption habits, new technologies, economic developments, environmental and geographical restrictions, greater demands on reliability, and quality, among others [1]. As a consequence of this, the electrical infrastructure is oversized, there are suboptimal decisions in this cycle, the planning objectives are opposed, and new operational constraints appear; for that reason, operational diagnoses in regular intervals during the useful life of a network are necessary. The network architecture must be reassessed with the help of optimization techniques to achieve economic and reliable operation [3]. In

Abbreviations: CDF, Customer Damage Function; CENTROSUR, "Empresa Eléctrica Regional Centro Sur C.A."; FEA, Failure Effect Analysis; IEEE, The Institute of Electrical and Electronics Engineers, Inc.; ISO, Independent System Operator; LC, Large Customer; NSGA-II, Nondominated Sorting Genetic Algorithm II; OTS, Optimal Transmission Switching; OSTS, Optimal Sub-Transmission Switching; SCADA, Supervisory Control And Data Acquisition; S/E, Substation.

* Corresponding author: Av. Max Ulhe y Pumapungo, CENTROSUR, 010209, Cuenca, Azuay, Ecuador
E-mail address: sergiopza.24@gmail.com (Z.-A. Sergio).

https://doi.org/10.1016/j.epsr.2022.108068
Received 2 December 2021; Received in revised form 18 April 2022; Accepted 4 May 2022
Available online 14 May 2022

Nomenclature

Sets

Ω_b	set of nodes
Ω_c	set of customer types
Ω_d	set of load levels
Ω_g	set of generators
Ω_k	set of contingencies
Ω_l	set of lines
Ω_{lp}	set of load points
Ω_t	set of transformers

Parameters

Acc	Accuracy parameter
Closs	Losses cost
$\overline{I_i}$	Thermal power flow limit in each subtransmission line i
Nsl	Maximum number of lines to be switched
$\overline{P_i}$	Maximum operating power for each transformer i
$\underline{V}$	Lower voltage limit
$\overline{V}$	Upper voltage limit
$\widehat{T}$	Hours per year

Variables

ACIF	Average customer interruption frequency
ACIT	Average customer interruption time
ASAI	Average system availability index
C_j	Consumers supplied by load point j
EENS	Expected energy not supplied
EIC	Expected interruption cost
EIC_d	Expected interruption cost at load level d
$frac_{j,k}$	Fraction of the load which is lost at load point j, for contingency k
Fr_k	Frequency of occurrence of contingency k
ICDF	Individual customer damage function
IEAR	Interrupted energy assessment rate
L_i	Load value at hour i
L_{int}	Load interval
L_d	Load value in the level d
L_{max}	Maximum value of each load
LPCDF	Load point customer damage function
LPEIC	Load point interruption cost
LPENS	Load point energy not supplied
n_d	Number of hours in load level d
$\widehat{Pd_j}$	Power disconnected at load point j
$Ploss_{l,d}$	Power losses of lines l for load level d
$Ploss_{t,d}$	Power losses of transformers t for load level d
$\widehat{Ps_j}$	Power shed at load point j
$p(d)$	Probability of load level d
Pr_k	Probability of occurrence of contingency k
SAIFI	System average interruption frequency index
SAIDI	System average interruption duration index
x_i	Binary variable that depends on the configuration proposed for line i, whether it is open or closed.
θ_i	Energization of load i
β_i	Energization of generator i
γ_i	Intentional islanded operation of generator i

Units

1/y	times a year
km	kilometer
km^2	Square kilometer
kV	kilovolts
kWh	kilowatt hour
GWh	Gigawatt hour
h/y	hours / year
min	minutes
MW	Megawatt
MWh	Megawatt hour
Ω	ohms
p.u.	per unit
USD	United States Dollar
USD/kW	USD / kilowatt
USD/kWh	USD / kilowatt hour

operational planning this problem is known as optimal switching.

The goal of the optimal switching is not to satisfy long-term reliability or capacity criteria, but rather to optimize a topology under current -or short-term forecast- network conditions [4]. This optimization of the topology takes advantage of the switching capability of the circuit breakers for a better use of the existing system [5], under a concept of a more active and technologically mature network. Most of the publications on the optimal switching problem have been addressed for the transmission system and include generation dispatch; this problem is known as optimal transmission switching (OTS) [4]. For the purposes of practical application of the OTS, it is expected that the number of switched lines is not high [6].

In meshed networks, there could be violations of the capacity limits of lines and transformers, which can be solved by disconnecting some lines in order to redirect the load flow. In OTS problems this is known as Braess's paradox; models that explain and justify this occurrence are proposed in [7]. An explanation of why the disconnection of a transmission line could improve the performance of the system, even when transmission capacity is lost, is made in [8] based on Kirchhoff's voltage law.

Heuristics have been used to find high-quality feasible solutions for the OTS problem, either to reduce solving times for practical use [9] or because commercial solvers may not be able to solve these problems [10]. Furthermore, meta-heuristic based algorithms are being used for the OTS problem, which are well suited to the non-linear nature with combination of real and binary variables [11,12]. Thus, particle swarm optimization has been used to solve a multi-objective version of the transmission topology and generation dispatch, by converting the problem into a single-objective function [11]. The multi-objective probabilistic solution discovery algorithm MO-PSDA was used in [11] to determine the optimal dispatch through a DC power flow and calculate the unserved load using Monte Carlo scenarios.

The OTS problem has been addressed through multi-objective optimization, including reliability, which is a highly relevant objective for the network planner. A multi-objective optimization approach was used in [11] to find OTS strategies minimizing generation cost and maximizing reliability considering the failure probabilities of components and quantifying their impact on reliability. To avoid compromising the safety of the transmission system, [13] proposes a formulation based on the optimal ac power flow, followed sequentially by an N-1 contingency analysis.

Reliability assessment is traditionally performed with simulation-based [14,15] or analytical methods [16] and, currently, optimization model-based methods are used [17]. In these last models, a post-fault network reconfiguration [18], or also called failure effect analysis (FEA), was used in semi-active networks under radial operation [19]. Reliability assessment can be integrated it into the network expansion and operational planning models as a constraint or as part of the

objective function (e.g., a cost to provide reliability and the incurred costs associated with interruptions [20]). Today, utilities require reliability-based planning by solving multiobjective optimization problems, and those who already apply it observe that they are far from the Pareto optimality front [20].

Moreover, utilities need a cyclical process to evaluate the operation based on the current conditions of the network architecture. This is one of the first works that addresses the problem of optimal switching for a subtransmission system. One of the few works that analyzes the subtransmission system is [21]; however, its main focus is the reconfiguration of primary distribution networks, minimizing losses and the number of interrupted consumers. In order to find an optimal operating point of the subtransmission system, considering distribution switching actions, [22] uses an alternating current-optimal power flow (AC-OPF). This approach is not exactly an optimal switching and does not consider the variability of the generation connected to the subtransmission system, nor the contingencies, and even less the quantification of reliability costs.

In this paper an optimal subtransmission switching (OSTS) approach is proposed for the economical and reliable operation of a subtransmission network. The objective function is composed of the operational costs related to energy losses and the reliability related to expected interruption cost. The nondominated sorting genetic algorithm II (NSGA-II) [23] will be used to solve the constrained multi-objective OSTS problem. A hierarchical coupling of a simulation-based optimization framework is built to find an approximation of the Pareto front. Due to the complexity of the problem, this work uses a reliability simulation method for fully meshed operation in subtransmission networks with multiple-point feeding, considering the logic of circuit breaker protections and the FEA. The main contributions of this work are as follows:

- One of the first optimization frameworks for the OSTS problem.
- The minimization of the expected interruption cost that is associated with the energy not supplied and the customer damage function is considered in the reliability evaluation. Probabilistic contingency assessment incorporates failure effect analysis including fault clearance, fault separation, and power restoration by opening and closing switches.
- The use of a simulation-based optimization coupling hierarchical framework to solve a constrained multi-objective problem.
- A real subtransmission system is used to evaluate the proposed framework, which corresponds to a meshed network with multiple feeding points to the transmission system.

2. BACKGROUND

The nature of the OSTS problem is nonlinear, mixed-integer, with stochastic variables and multiple conflicting planning objectives; also, the meshed network operating with multiple-points feeding increases the complexity of this NP-hard problem. This motivates the development of optimization strategies coupled with simulation for its solution. Here, simulation-based optimization is adopted along with the metaheuristic NSGA-II for the solution of the OSTS problem.

2.1. Differences between the OSTS and OTS problem

According to the discussion above, the growth of the subtransmission system is initially influenced by contingency-based planning and requires a reliability assessment for both expansion and operation. There are common characteristics between a transmission and subtransmission system, related to their switching capabilities, but the latter requires a more detailed reliability evaluation [24] since it articulates a primary distribution system and needs to provide greater operational flexibility. The subtransmission network, being part of a distribution system, requires high quality and reliability because a failure causes a high impact on the consumer interruption costs.

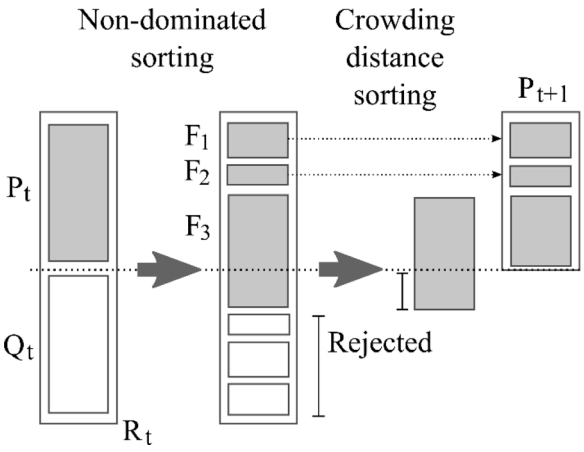

Fig. 1. NSGA-II procedure [23].

The definition and evaluation of reliability between generation and distribution systems is totally different. In OTS problems, the reliability cost relates to generation reserve capacity, commonly evaluated by loss of load probability (LOLP), or loss of load expectation (LOLE) [11]. As will be presented later, consumer-oriented reliability indices [25] are used for the subtransmission system, whose interruption costs are characterized by consumption sector. Therefore, this paper includes, as an objective of an OSTS approach, the social value of electric service reliability in subtransmission systems through the expected interruption cost [26].

2.2. Simulation-based optimization

Co-simulation techniques allow a global simulation combining different simulators in which each one represents a black box developed by experts [27]; for example, OpenDSS and GridLab-D are widely used open-source distribution system simulators, while DIgSILENT PowerFactory [28] is an industrial package for power system analysis. Optimization tools coupled to simulators have significant potential in the integrated planning and operation of transmission and distribution systems [27]. That simulation-based optimization is an automated process that iteratively approximates a solution up to satisfying an optimality condition [29]. There are mainly two types of coupling in simulation-based optimization: sequential and hierarchical [30]. In the hierarchical coupling adopted in this proposal, the optimization method controls the simulation to evaluate the dynamic behavior of the subtransmission system.

Some application cases of this coupled framework are in building performance analysis (e.g., net zero-energy buildings) [29], operation and dispatch optimization of unbalanced active distribution system [31], coordinated tuning of power system supplementary damping controllers [32], severe weather events that can trigger cascading power outages [33], transmission network expansion planning [34], among others.

2.3. Brief description of NSGA-II

NSGA-II is a constrained multi-objective evolutionary algorithm that uses a fast non-dominated sorting approach to identify non-dominated Pareto fronts [23]. The population is classified in different levels of non-dominance; a fitness value equal to the nondomination level is assigned to each solution. Diversity between non-dominated solutions uses a crowded-comparison approach in which a density-estimation metric and a crowded-comparison operator are defined [23]. The solutions compete through this crowding-distance both in the tournament selection and in the population reduction phase. The NSGA-II procedure

Algorithm 1
NSGA-II procedure [35]

1: Create a random parent population P_0 of size N. Set $t = 0$.
2: Apply crossover and mutation to P_0 to create offspring population Q_0 of size N.
3: If the stopping criterion is satisfied, stop and return P_t.
4: Set $R_t = P_t \cup Q_t$.
5: Use the fast non-dominated sorting algorithm to identify the non-dominated fronts $F_1, F_2, \ldots, F_k$ in R_t.
6: For $i = 1, \ldots, k$ do:
6.1: Calculate crowding distance of the solutions in F_i
6.2: Create P_{t+1} as follows:
Case 1: If $|P_{t+1}| + |F_i| \leq N$, then set $P_{t+1} = P_{t+1} \cup F_i$;
Case 2: If $|P_{t+1}| + |F_i| > N$, then add the least crowded $N - |P_{t+1}|$ solutions from F_i to P_{t+1}.
7: Use binary tournament selection based on the rank and crowding distance to select parents from P_{t+1}. Apply crossover and mutation to P_{t+1} to create offspring population Q_{t+1} of size N.
8: Set $t = t + 1$ and go to step 3.

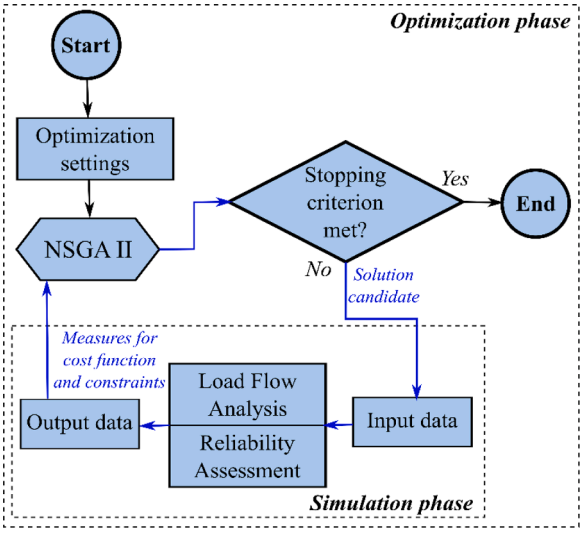

Fig. 2. Simulation-based optimization coupling hierarchical framework for the OSTS problem.

is shown in Fig. 1 and detailed in Algorithm 1.

To represent line switching, the OSTS problem is coded as a vector of zeros and ones, where one represents switching or opening a line. This vector is made up only of subtransmission lines that are part of the meshed network. The NSGA-II will create feasible solution proposals based on this coding structure.

2.4. Simulation software

PowerFactory [28] is a power system analysis software that includes load flow simulation and reliability assessment; it has been chosen for the simulation phase of the proposed method. To model the failure behavior of the system components, PowerFactory uses different models, such as Weibull–Markov [14]. Additionally, the reliability analysis incorporates FEA and maintenance plans; it also can incorporate different load levels. FEA includes fault clearance, fault separation and power restoration by opening and closing switches, overload alleviation and voltage restrictions alleviation by load transfers, and load shedding [36].

PowerFactory was developed to analyze in detail the reliability in large power systems [37]. However, the challenges are the adequacy of input information, as well as reusing its functions within optimization or simulation frameworks to add more potential to the analysis. A versatile tool to extend the functionality of PowerFactory is Python, which allows the construction of applications whose limits are the creativity of the user [38]. In the proposed method, the dynamic Python module ("powerfactory.pyd") [36] is used to interact with the PowerFactory API (Application Programming Interface) [39] and execute it externally as a black box.

3. PROPOSED METHOD FOR THE OSTS PROBLEM

The OSTS problem is formulated as a constrained multi-objective optimization considering operational cost and expected interruption cost. The goal is to obtain a set of non-dominated solutions that form the Pareto front, so that the planner decides an economic and reliable operating condition based on their priorities and needs. Due to the complexity of the problem, the widely known NSGA-II algorithm is used to find good quality solutions. For this, the hierarchical coupling of a simulation-based optimization framework, shown in Fig. 2, is built. The simulation is used to calculate the objective function and constraints; hence the optimization performs the alternative search for candidate solutions.

3.1. Load levels

Load levels are defined to manage uncertainty and seasonal vari-

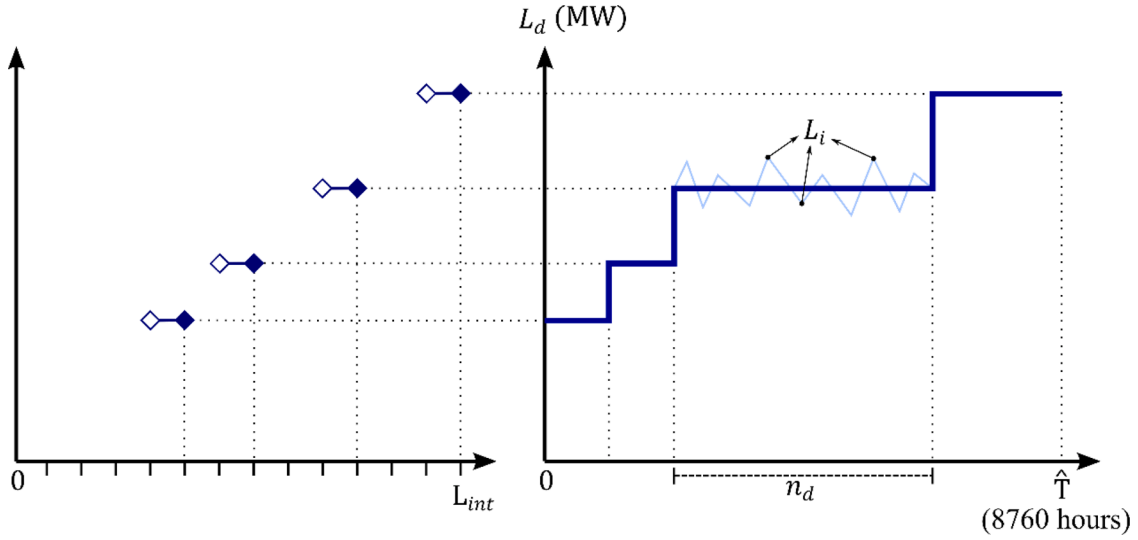

Fig. 3. Construction of load levels for an annual series.

ability both for generation plants and load points. In this research a **"load point"** represents the concentration of consumers and loads within a service area of a medium-voltage feeder. The time-based parameter characteristics (hourly values) of loads are considered to calculate the load intervals through (1).

$$L_{int} = Ceil\left(\frac{L_i}{L_{max}\cdot Acc}\right) \ \forall i \in \{1,\ldots,\widehat{\mathrm{T}}\} \tag{1}$$

where L_{int} is the load interval, L_i is the load value at hour i, L_{max} is the maximum value of each load, and Acc is the accuracy parameter (expressed in %). $Ceil()$ is a function that returns the smallest integer value that is bigger than or equal to the given number. The total number of hours per year is represented as $\widehat{\mathrm{T}}$ (8,760 hours).

The set of load levels Ω_d depends on the accuracy parameter Acc and the lower its value, the more load levels are generated. The frequency of occurrence of the load intervals determines the probability of each load level, as defined by (2).

$$p(d) = \frac{n_d}{\widehat{\mathrm{T}}} \tag{2}$$

where $p(d)$ is the probability of load level d and n_d is the number of hours in the load level d. Thus, the value of the load of each level is represented in (3) by the mean.

$$L_d = \frac{1}{n_d}\sum_{i\in n_d} L_i \tag{3}$$

Fig. 3 graphically illustrates the procedure for the construction of the load levels for a given accuracy. The right graph shows 4 load levels, with the respective duration n_d of the interval. Each load interval L_{int} was defined with the $Ceil()$ function, where the corresponding class is presented in the left graph. In addition, in interval 3, the load values L_i are presented, whose average demand for all the hours of the interval is represented by the blue bold line.

3.2. Reliability assessment

The reliability of a subtransmission/distribution system is associated with the performance and continuity of the electrical service at the load point level [25]. Continuity between supply points and load points depends not only on component-related failures, but also on the operating logic of protection equipment and the optimal configuration of the subtransmission system. The optimization model uses the reliability indices at the system level, which are deduced from the reliability indexes at the load point level.

3.2.1. Load point indices

Reliability analysis is a probabilistic extension of contingency assessment and considers stochastic failure and repair models to generate reliability indices [36]. The reliability parameters of the system's components, such as lines, transformers, buses, switching and protection equipment, etc., are basically the failure rate and the repair time, generally obtained from a statistical analysis. Here, the components are represented with two states of availability: "in service" and "under repair".

The two main indices for the load points Ω_{lp} are average customer interruption frequency (ACIF) defined in (4), and average customer interruption time (ACIT) defined in (5). They depend on the frequency of occurrence of contingency k ($\mathrm{Fr_k}$), and the probability of occurrence of contingency k (Pr_k).

$$ACIF_j = \sum_{k\in\Omega_k} Fr_k\cdot frac_{j,k} \ \forall j \in \Omega_{lp} \tag{4}$$

$$ACIT_j = \sum_{k\in\Omega_k} \widehat{\mathrm{T}}\cdot Pr_k\cdot frac_{j,k} \ \forall j \in \Omega_{lp} \tag{5}$$

$$0 \le frac_{j,k} < 1 \tag{6}$$

where $frac_{j,k}$ is the fraction of the load lost at load point j, for contingency k. For unsupplied loads or for loads that are completely shed, $frac_{j,k} = 1$.

From (5), the load point energy not supplied $LPENS_j$ at load point j is defined in (7).

$$LPENS_j = ACIT_j\cdot\left(\widehat{Pd}_j + \widehat{Ps}_j\right) \ \forall j \in \Omega_{lp} \tag{7}$$

where $\widehat{Pd}_j$ is the weighted average amount of power disconnected at load point j, and $\widehat{Ps}_j$ is the weighted average amount of power shed at load point j.

3.2.2. Load point interruption cost

The load point interruption cost (LPEIC) at load point j depends on contingency k, according to (8). This is also associated with the energy not supplied and the customer damage function (CDF).

$$LPEIC_j = \sum_{k\in\Omega_k} LPEIC_{j,k} \ \forall j \in \Omega_{lp} \tag{8}$$

The CDF represents the costs incurred during an interruption related to the inability of customers to carry out their activities [40]. At each load point, there is a composition of various types of customers; thus, the load point customer damage function (LPCDF) is determined in (9) using individual CDFs (ICDF) [40,41], which are a function of the interruption's duration.

$$LPCDF_j = \sum_{l\in\Omega_c} w_l\cdot ICDF_l(\delta_k) \ \forall j \in \Omega_{lp}, \ \forall k \in \Omega_k \tag{9}$$

where w_l is the percentage of energy curtailed for customer type l, $ICDF_l$ is the individual CDF for consumer type l, and δ_k is the interruption duration for contingency k.

3.2.3. System indices

System indices are adopted to assess the general performance of the system; they are derived from the basic indices at the load point level [15]. The most commonly system indices for sustained interruptions defined in the reliability guide IEEE Std. 1366-2012 [42] are system average interruption frequency index (SAIFI), system average interruption duration index (SAIDI), and average system availability index (ASAI). Equations (10)–(12) define these indices as a function of the load point indices and the number of consumers C_j supplied by load point j.

$$SAIFI = \frac{\sum_{j\in\Omega_{lp}} ACIF_j\cdot C_j}{\sum_{j\in\Omega_{lp}} C_j} \tag{10}$$

$$SAIDI = \frac{\sum_{j\in\Omega_{lp}} ACIT_j\cdot C_j}{\sum_{j\in\Omega_{lp}} C_j} \tag{11}$$

$$ASAI = \frac{\widehat{\mathrm{T}}\cdot\sum_{j\in\Omega_{lp}} C_j - \sum_{j\in\Omega_{lp}} ACIT_j\cdot C_j}{\widehat{\mathrm{T}}\cdot\sum_{j\in\Omega_{lp}} C_j} \tag{12}$$

The expected energy not supplied (EENS) in (13) links the unreliability of the system with the reliability worth [25]. Since an explicit cost to evaluate the reliability is used in the decision-making process, the expected interruption cost (EIC), defined in (14), is adopted. The relation between the latter two is known as the interrupted energy assessment rate (IEAR), calculated by (15).

$$EENS = \sum_{j\in\Omega_{lp}} LPENS_j \tag{13}$$

$$EIC = \sum_{j\in\Omega_{lp}} LPEIC_j \tag{14}$$

$$IEAR = \frac{EIC}{EENS} \tag{15}$$

3.3. Objective function

The objective function considers two conflicting objectives, i.e., to minimize energy losses by seeking economic operation and to minimize the expected interruption cost by pursuing reliable operation.

3.3.1. Minimization of the losses cost

The cost of energy losses is a typical operating cost in the provision of electricity supply. This cost constitutes the first objective to be minimized in (16), considering the losses in lines and in power transformers for each load level. That calculation depends on the total number of hours per year and the probability $p(d)$ of load level d.

$$Min\, f_1 = \hat{T}\sum_{d\in\Omega_d} p(d)\cdot Closs\left(\sum_{l\in\Omega_l} Ploss_{l,d}\cdot x_l + \sum_{t\in\Omega_t} Ploss_{t,d}\right) \tag{16}$$

$$x_l = \begin{cases} 0 \text{ if the line } 'l' \text{ is switched off} \\ 1 \text{ if the line } 'l' \text{ is closed} \end{cases} \tag{17}$$

where $Closs$ is the losses cost, $Ploss_{l,d}$ and $Ploss_{t,d}$ are the power losses of lines l and transformers t, respectively, for load level d. The binary variable x_l depends on the proposed configuration of the network topology, i.e., whether the subtransmission line l is open or closed.

3.3.2. Minimization of the expected interruption cost

The second conflicting objective that evaluates reliability in (18), considers the minimization of the EIC of the system for the established load levels. That calculation depends on the total number of hours per year, the probability $p(d)$ of load level d, and the expected interruption cost at load level d (EIC_d).

$$Min\, f_2 = \hat{T}\sum_{d\in\Omega_d} p(d)\cdot EIC_d \tag{18}$$

3.4. Constraints

The first set of constraints guarantee the satisfaction of the operational limits, while the second group ensures that all loads and generators are energized without the formation of intentional islands. The voltage in each bus must be within a generally defined regulation range, as shown in (19), where $\underline{V}$ is the lower limit and $\overline{V}$ is the upper limit. The thermal limit in each subtransmission line is given by $\overline{I_i}$, according to (20). The maximum operating power for each transformer is given by (21); under conservative planning criteria, a reserve capacity is usually left associated with its ONAN / ONAF (Oil Natural Air Natural / Oil Natural Air Forced) capacity. Furthermore, (21) guarantees the energization of all the loads, $\theta_i = 0$ if the load i does not have electricity supply, while $\theta_i = 1$ if the load i is served. Analogously to the previous constraint, (23) enforces that all generators are energized; thus, if a generator i is not energized, then $\beta_i = 0$, leading to the violation of the constraint. Although there may be generation units that have black start and frequency regulation, the formation of an intentional island in the normal operation of the subtransmission system is not desirable; this is avoided by (24), in which $\gamma_i = 1$ indicates that generator i is forming an island. Finally, restriction (25) constitutes a strategy to speed up processing, since it is not desirable that too many lines be disconnected, and Nsl represents the maximum number of lines to be switched.

$$\underline{V} \le V_i \le \overline{V}\ \forall i \in \Omega_b \tag{19}$$

$$I_i\cdot x_i \le \overline{I_i}\ \forall i \in \Omega_l \tag{20}$$

Table 1
Energy and power demand by substation and large consumers of the subtransmission system.

Substation / Large consumer	Feeders	Peak Load [MW]	Annual Energy [GWh]	Customers
S/E 01	4	5.93	32.01	12,885
S/E 02	5	7.19	41.77	10,406
S/E 03	5	22.01	95.49	45,143
S/E 04	9	34.85	176.60	33,398
S/E 05	10	35.95	197.57	78,515
S/E 07	3	15.58	79.78	22,962
S/E 08	4	22.75	70.56	24,575
S/E 09	1	2.50	12.97	9,658
S/E 12	3	9.37	38.32	17,934
S/E 13	1	1.10	5.36	15
S/E 14	4	11.97	63.12	30,653
S/E 15	3	10.66	49.54	36,603
S/E 18	4	8.41	42.42	26,241
S/E 21	6	9.84	53.28	20,960
S/E 22	3	3.04	15.38	6,632
S/E 23	2	1.59	7.60	4,585
LC 01	-	6.44	30.36	1
LC 02	-	12.58	53.93	1
S/E A1	4	15.01	34.88	21,581
S/E A2	4	11.60	34.97	16,671
LC 03	-	8.15	44.04	1
Total	**75**	**256.52**	**1,179.94**	**419,420**

$$P_i \le \overline{P_i}\ \forall i \in \Omega_t \tag{21}$$

$$\prod_{i\in\Omega_{lp}} \theta_i = 1 \tag{22}$$

$$\prod_{i\in\Omega_g} \beta_i = 1 \tag{23}$$

$$\sum_{i\in\Omega_g} \gamma_i = 0 \tag{24}$$

$$\sum_{i\in\Omega_l} (1 - x_i) \le Nsl \tag{25}$$

4. CASE STUDY

The proposed approach was applied to the electrical subtransmission system of the "Empresa Eléctrica Regional Centro Sur C.A." (CENTROSUR), located in Cuenca, Ecuador. The service area of CENTROSUR is 30,234 km^2 (11.8% of Ecuadorian territory) and the annual energy consumption of its 419,420 customers in 2019 (88% residential, 11% commercial, and 1% industrial) was 1,179.94 GWh (Table 1).

The subtransmission network, illustrated in Fig. 4, has two feeding points from the transmission system at both 138 kV and 230 kV. The meshed grid is mainly at the 69 kV level, whose lines are considered in the switching optimization problem. The subtransmission system is strongly influenced by the bulk power system, causing an angular voltage gradient between both feeding points.

The load is distributed in 18 substations (S/E) and 3 large industrial energy consumers (LC), as detailed in Table 1. Two of the substations (S/E A1 and S/E A2) and one large consumer (LC 03) are part of a nearby distribution utility integrated into the subtransmission system. The loads in each substation correspond to the medium-voltage feeders, simplified as a single load in Fig. 4. Additionally, there are 6 power generation plants distributed in the subtransmission network, mainly hydroelectric power, described in Table 2.

The subtransmission system is made up of 39 lines whose characteristics are detailed in Table 3. There are 4 lines at the 22 kV level that feed substations S/E 01 and S/E 02, which serve the historic center of the city, being 3 of them underground (dashed line in Fig. 4). The details of

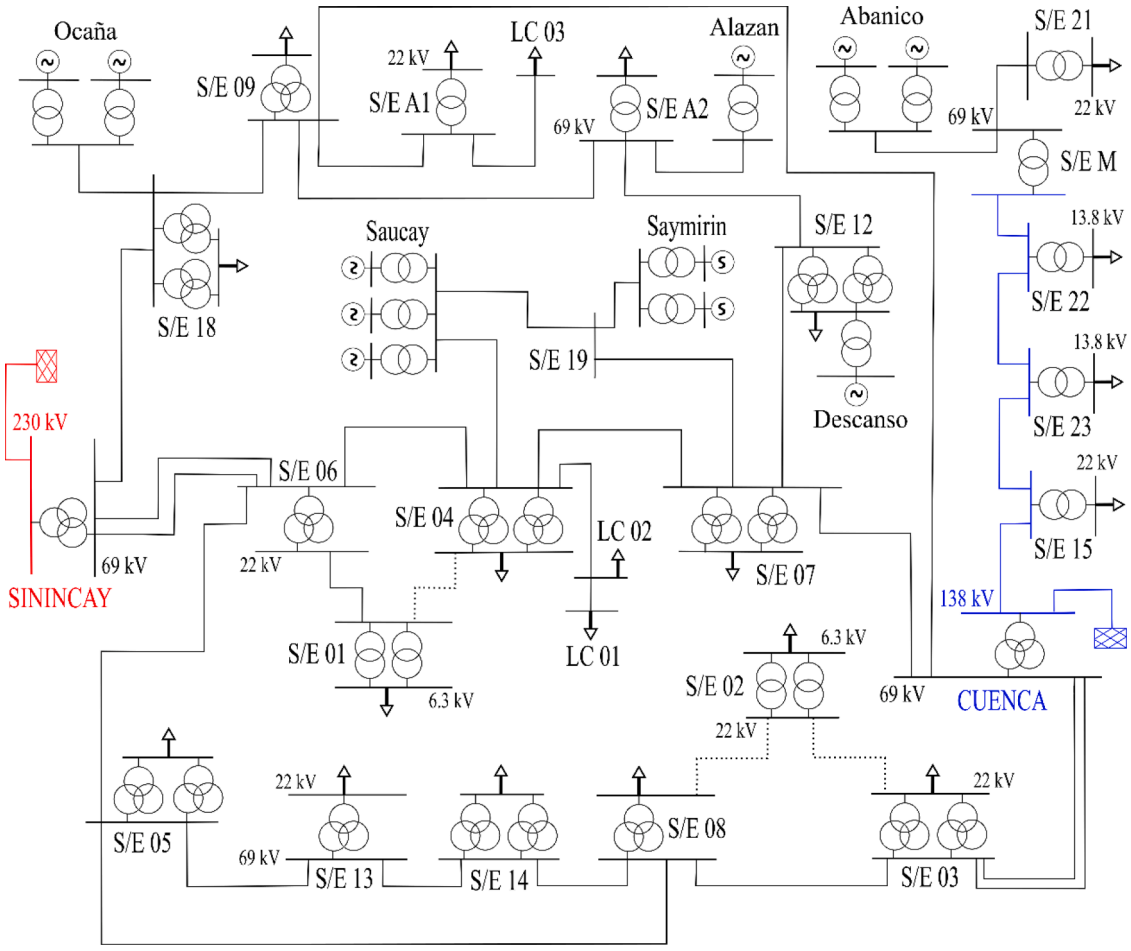

Fig. 4. Subtransmission network of the Electric Distribution Utility, Cuenca – Ecuador.

Table 2
Distributed generation plants in the subtransmission system

Generation plant	Type	Units	Power [MW]	Annual Energy [GWh]
Descanso	fossil fuel	4	15.92	3.41
Abanico	hydro	5	37.65	266.40
Ocaña	hydro	2	26.56	204.13
Saucay	hydro	4	23.60	109.11
Saymirin	hydro	4	15.76	93.64
Alazan	hydro	1	4.52	26.99
Total		**20**	**124.01**	**703.69**

the parameters of three-winding and two-winding transformers are presented in Appendix A.

The proposed simulation-based optimization framework was built with the Python 3.8 language interacting with the PowerFactory API (version 2021 SP4). Python function acceleration strategies from the Numba library were also used.

4.1. Costs of interruptions and losses

To quantify reliability in monetary units, several surveys and studies were carried out to evaluate the CDF of a large number of countries [40]. That data is commonly used to determine capacity payments, expansion planning, network design, security standards, among others.

Table 4 shows the CDFs by sector taken from [41], which are used in this case study to approximate the EIC of the subtransmission system. It is worth to note that commercial customers have the highest CDF values.

In order to simplify the calculation of interruption costs, a general LPCDF is determined using (9), considering the ICDF in Table 4, and using a weighting factor by sector based on annual energy consumption. The weights by customer type for the case study are: Residential=42.00%, Commercial=16.58%, Industrial=33.86%, and Gov&Inst.=7.56%. With that information, the cost curve is built as a function of the interruption duration (see Fig. 5).

On the other hand, the cost of losses is established based on the electricity price that the electric distribution utility buys in the wholesale electricity market. This price is mainly influenced by the construction and operation of large hydroelectric generation plants in recent years [43]. A value of 24.2 USD/MWh was adopted.

4.2. Load model

To build the load and generation levels, SCADA measurement information corresponding to a full year was utilized. Feeder 0421 of S/E 04, which covers part of an industrial zone, will be used to exemplify the creation of load levels. Fig. 6a shows the hourly feeder load profile for the year 2019 (observed the limited seasonal variation). With an accuracy Acc = 20% and neglecting load values with probabilities below 5%, Fig. 6b shows the three load states with their associated probability.

By combining the 75 feeders and the 20 generation units of the subtransmission network, d = 4 load levels are obtained with the following probabilities $p(d)$: 0.6207, 0.1376, 0.1284, and 0.1133. For each load level, active and reactive powers were obtained, which is the input to evaluate the reliability and simulate the load flow.

Table 3
Lines of the subtransmission system

Line	From	To	Length [km]	Voltage [kV]	R [Ω]	X [Ω]
1	SININCAY	S/E 06	8.0	69	0.90	3.25
2	SININCAY	S/E 06	8.2	69	0.92	3.31
3	SININCAY	S/E 18	31.7	69	3.56	12.85
4	CUENCA	S/E 03	3.4	69	0.43	1.42
5	CUENCA	S/E 03	3.0	69	0.42	1.38
6	CUENCA	S/E 07	5.3	69	0.75	2.22
7	CUENCA	S/E 09	23.8	69	3.34	10.49
8	S/E 05	S/E 13	11.1	69	2.76	5.25
9	S/E 05	S/E 08	5.1	69	0.72	2.28
10	S/E 03	S/E 02	1.5	22	0.16	0.17
11	S/E 03	S/E 08	4.5	69	0.63	2.01
12	S/E 18	Ocaña	42.0	69	5.19	19.47
13	S/E 04	LC 02	1.9	69	0.47	0.81
14	LC 02	LC 01	0.2	69	0.05	0.09
15	S/E 04	S/E 07	3.8	69	0.43	1.55
16	S/E 04	Saucay	14.1	69	1.98	6.27
17	S/E 04	S/E 01	2.7	22	0.62	1.17
18	S/E 07	S/E 12	10.2	69	2.55	4.71
19	S/E 13	S/E 14	36.5	69	9.10	17.33
20	S/E 09	S/E 18	24.1	69	6.03	11.56
21	S/E 09	S/E A1	0.9	69	0.12	0.38
22	S/E A1	LC 03	2.5	69	0.35	1.13
23	S/E 09	S/E A2	1.7	69	0.24	0.76
24	S/E A2	Alazan	34.7	69	4.16	12.40
25	S/E 12	S/E A2	10.3	69	1.44	4.52
26	S/E 07	S/E 19	9.9	69	1.38	4.41
27	S/E 19	Saymirin	1.3	69	0.19	0.61
28	S/E 19	Saucay	4.9	69	0.69	2.17
29	S/E 08	S/E 14	45.6	69	5.14	18.52
30	S/E 08	S/E 02	4.0	22	0.40	0.45
31	S/E 06	S/E 05	7.2	69	0.81	2.92
32	S/E 06	S/E 04	3.2	69	0.36	1.31
33	S/E 06	S/E 01	1.4	22	0.32	0.60
34	CUENCA	S/E 15	21.0	138	5.28	10.80
35	S/E 15	S/E 23	45.5	138	11.96	24.40
36	S/E 23	S/E 22	33.0	138	8.20	16.13
37	S/E 22	S/E M	51.7	138	12.75	24.56
38	S/E M	S/E 21	0.1	69	0.03	0.05
39	S/E M	Abanico	11.5	69	1.60	4.44

Table 4
Individual customer damage functions ($/kW) [41]

Sector	1 min	20 min	60 min	240 min	480 min
Residential	0.0000	0.0278	0.1626	1.8126	4.0006
Commercial	0.9797	11.8537	35.1409	166.2123	305.2044
Industrial	1.8808	4.7237	12.2565	46.3678	88.5821
Gov&Inst.	1.0317	9.5468	20.7244	77.7868	153.8700

4.3. Results of the optimization model

The failure rate and repair time for overhead and underground lines of the sub-transmission system was determined by taking advantage of utility statistics. For protection equipment and power transformers, these data were taken from specialized literature [44]. Moreover, failure rate and repair time were not considered for the generation units, whose dispatch obeys the scheduling of the independent system operator (ISO).

In theory there are 2^{39} (549,755,813,888) possible solutions, according to the number of lines in Table 3; however, the solutions are not expected to have a significant number of switched lines, due to constraints and the two conflicting objectives. Strategically, the energization restrictions of loads and generators are evaluated before the load flow and reliability calculation aiming to restrict the search space and optimize time. The NSGA-II was set with a random initial population of 5,000 configurations, being 1,300 feasible solutions. The minimum population size is 90 and its maximum size is 180; a mutation probability of 0.01 was used. The maximum number of iterations was defined as 600 for the stopping criterion. Furthermore, the PowerFactory was

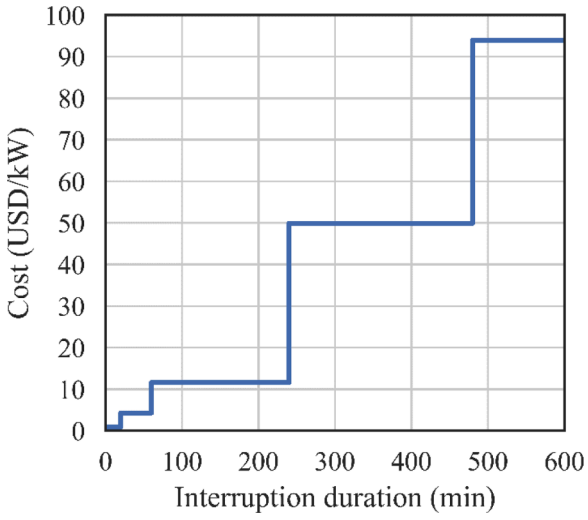

Fig. 5. LPCDF of the case of study.

configured to simulate balanced power flows, both for the evaluation of losses and operational restrictions, as well as to evaluate the reliability considering the FEA.

The stopping criterion was met after 104.35 hours of computing with a workstation with an Intel Xeon 3.60 GHz processor and 32 GB of RAM. The longest processing time of the framework proposed for this case study (with around 100 nodes) corresponds to the simulation phase, with an average of 1.35 seconds to evaluate the cost function and constraints for a feasible solution. For this run with 600 iterations, no maximum value of *Nsl* was established, thus the NSGA-II optimization algorithm evaluated hundreds of thousands of candidate solutions.

Fig. 7 shows a scatter plot of the final population, together with the Pareto front highlighted with the red line. The shape of the front is typical of a min-min optimization, with minimum values of USD-million 0.117 and USD-million 0.620 for EIC and loss costs, respectively. A maximum of 5 switched lines was found in the final population, while solutions with 3 switched lines were the most common (36 solutions).

4.4. Discussion

The discussion will be focused on 4 solutions of the Pareto front shown in Fig. 8. The analysis is based on the current topological configuration known as Base-case (blue color). Table 5 presents the detail of the switched lines (with the letter "X"); the omitted lines of the subtransmission system are closed. For these solutions, Table 6 also presents the reliability indices defined in the formulation, as well as the costs that are part of the two optimization objectives.

The Base case operates with three open subtransmission lines and, as can be seen in the Fig. 8, it is located above the Pareto front obtained. Solution 1 presents the lowest losses cost (Table 6); it sacrifices the reliability operating condition, which is undesirable due to the high EIC value. Solution 2 represents closing all the lines of the subtransmission system; it corresponds to the minimum reliability value (USD 116,808), as well as the global minimum. Compared with the Base case (Fig. 4), it indicates closing lines 30 and 33 to increase reliability in the historic center of the city. Solutions 3 and 4 correspond to the minimum value of the EIC, with a high ASAI index; their shifts to the right on the Pareto front cause a slight increase in the cost of annual losses, but bring other benefits discussed later.

To evaluate the benefits of the proposed decision-making tool, other needs of the operation planner are analyzed taking into account Solution 4. Fig. 9 shows the configuration of the subtransmission network after applying the switching of the three lines (highlighted in pink) established by this solution. As previously mentioned, multiple-point feeding

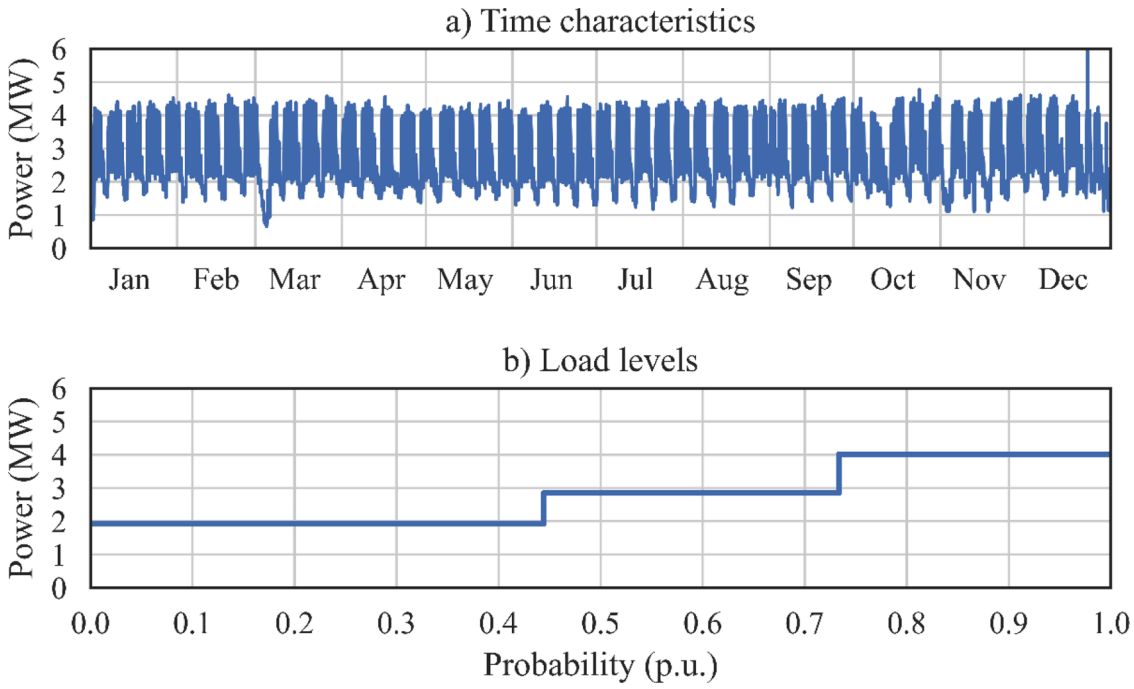

Fig. 6. Time characteristics and load levels of the Feeder 0421.

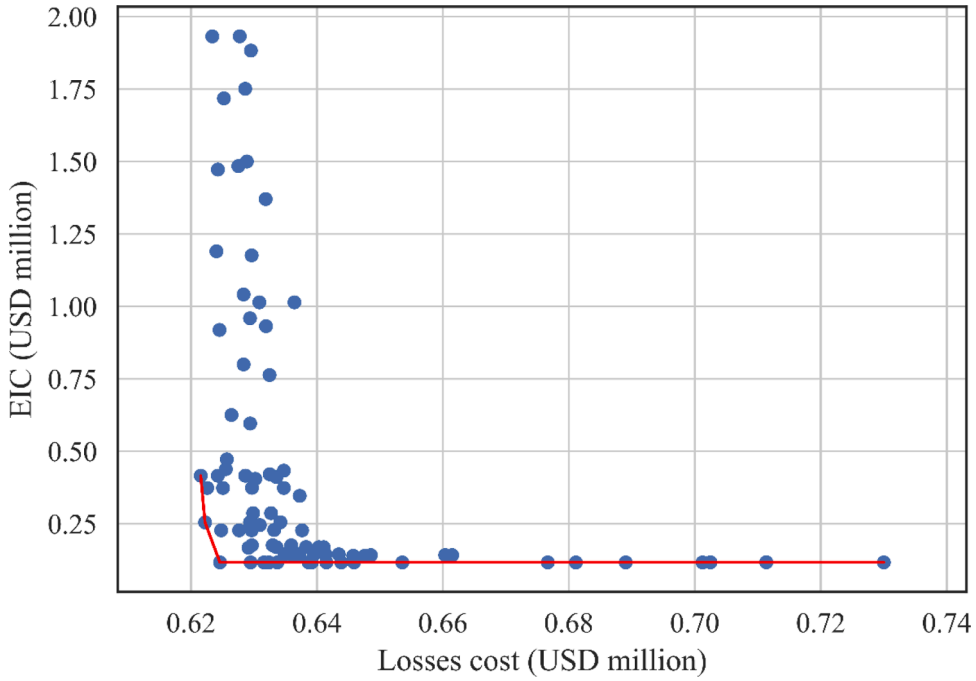

Fig. 7. Scatter plot of the final population and Pareto front (red line).

from the transmission system can impose constraints with the capacity of the transformers. Thus, the CUENCA substation transformer (138/69 kV) reaches a loading close to its nominal under normal operating conditions in the Base case and during peak demand hours, while the SININCAY substation transformer (230/69 kV) has an important reserve. In this way, it is not possible to inject more generation flow through the 138 kV transmission line, mainly in the contingency or emergency scenarios experienced by the ISO. Solution 4, in which reliability is optimized although with an increasing in losses, helps to solve the aforementioned problem. The loading of the transformer of the S/E CUENCA in Solution 4 is 22.64%, compared to 67.12% for the Base case; this is explained by the redistribution of the load flow.

Another important problem is that, in certain busbars of the subtransmission system, the short-circuit currents rise due to the decrease in impedance and generation contributions. By evaluating the set of solutions of the final population and the Pareto front, it was found that there are configurations that reduce these currents. For example, in the 22 kV bus of S/E 04, there are configurations that reduce these currents by 25% compared to the Base case. In this way, elite solutions, by meeting the optimization stopping criterion, also allow satisfying other needs or operational criteria, which could be part of the modeling or part of a subsequent analysis with another type of simulation such as short-

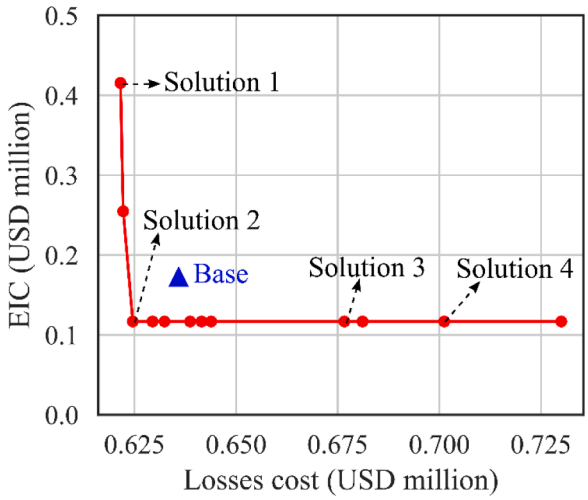

Fig. 8. Identification of solutions analyzed on the Pareto front.

circuits.

4.5. Performance of the NSGA-II algorithm

As mentioned above, more solutions with 3 switched lines are repeated in the final population obtained with NSGA-II algorithm. Therefore, a value of *Nsl*=4 in (25) was taken to evaluate an exhaustive search or brute force, in order to observe how close, the Pareto front found with NSGA-II is to the optimum. To speed up this search, radial lines were not considered either, such as the 138 kV subsystem, as well as the lines towards LCs in Fig. 4. Thus, the search space is reduced to tens of thousands of candidate solutions, notably reducing the time of this intensive search to 4.73 hours. Fig. 10 shows a scatter plot with 6,458 feasible solutions found by brute force; it also presents the Pareto optimal front of non-dominated solutions.

Fig. 11 shows the Pareto fronts obtained using the NSGA-II optimization algorithm and the exhaustive search, with a maximum of 4 switched lines. Fig. 11a shows the initial result of the NSGA-II algorithm; while Fig. 11b adds the restriction *Nsl* = 4 switched lines, with the parameters defined therein. In this way, the processing time of the metaheuristic is reduced to 3.23 hours for the present case study. Also, for comparison purposes, Fig. 11b shows another well-known multi-objective metaheuristic MOPSO based on the discrete binary of the particle swarm algorithm [45]. It is concluded that the Pareto front found with the proposed framework has good quality; there is even a high coincidence of the optimal reliability solutions (horizontal part of the curve). This confirms the wide application of the NSGA-II metaheuristic, concluding that it is highly suitable for the OSTS problem.

5. CONCLUSIONS

An optimal switching approach for the economical and reliable operation of subtransmission systems has been presented. A multi-objective optimization model that considers energy losses and reliability was formulated. A hierarchical coupling of a simulation-based optimization framework was built to solve the problem, i.e., the metaheuristic NSGA-II and a simulation method were joined to resolve load flow and assess reliability. The set of feasible solutions that make up the Pareto front constitutes a powerful decision-making tool for the planner to decide on an economic and reliable operating condition based on their priorities and needs.

In the case study with a real subtransmission system of an Ecuadorian power utility, some alternative solutions were compared with respect to the base case of operation, showing that it is highly recommended to switch certain strategic lines of the subtransmission system. The minimum value of the expected interruption cost and the range of variation of the losses cost were obtained, which allows the planner to define an operating condition. A subsequent analysis was also carried out with the solutions of the last iteration, based on additional overload needs in power transformers to the transmission system and the emerging of significant short-circuit currents. The latter shows the versatility of the proposed tool to explore operating conditions according to the needs, the dynamics of the subtransmission network, and the influence of the external transmission system.

To the best of the authors' knowledge, the proposal is one of the first approaches to solve the optimal switching problem for subtransmission systems including specific information of load characteristics, given that the specialized literature focused on transmission systems. Currently with the penetration of distributed energy resources, the primary and secondary distribution network is being very active, which will be reflected in the subtransmission network. Thus, this decision-making tool will be key to face such dynamics, which must be complemented with other tools, such as the timely calibration of protective equipment for

Table 5
Switched lines of some solutions of the Pareto front

Line [From - To]	Base	Solution 1	Solution 2	Solution 3	Solution 4
3 [SININCAY - S/E 18]	-	X	-	-	-
6 [CUENCA - S/E 07]	-	-	-	-	X
7 [CUENCA - S/E 09]	X	-	-	-	X
11 [S/E 03 - S/E 08]	-	-	-	X	X
30 [S/E 08 - S/E 02]	X	X	-	-	-
33 [S/E 06 - S/E 01]	X	-	-	-	-
Total switched lines	**3**	**2**	**0**	**1**	**3**

Table 6
Reliability indices and cost of some solutions of the Pareto front

Line [From - To]	Base	Solution 1	Solution 2	Solution 3	Solution 4
SAIFI (1/y)	0.013	0.081	0.007	0.176	0.177
SAIDI (h/y)	0.211	0.471	0.145	0.823	0.831
ASAI	0.999976	0.999946	0.999983	0.999906	0.999905
EENS (MWh/y)	25.95	45.04	17.17	93.09	94.16
IEAR (USD/kWh)	6.63	9.23	6.80	1.25	1.24
Losses cost (USD)	635,868	621,552	624,598	676,658	701,214
EIC (USD)	172,167	415,471	116,808	116,808	116,808
Total cost (USD)	**808,035**	**1,037,023**	**741,405**	**793,466**	**818,022**

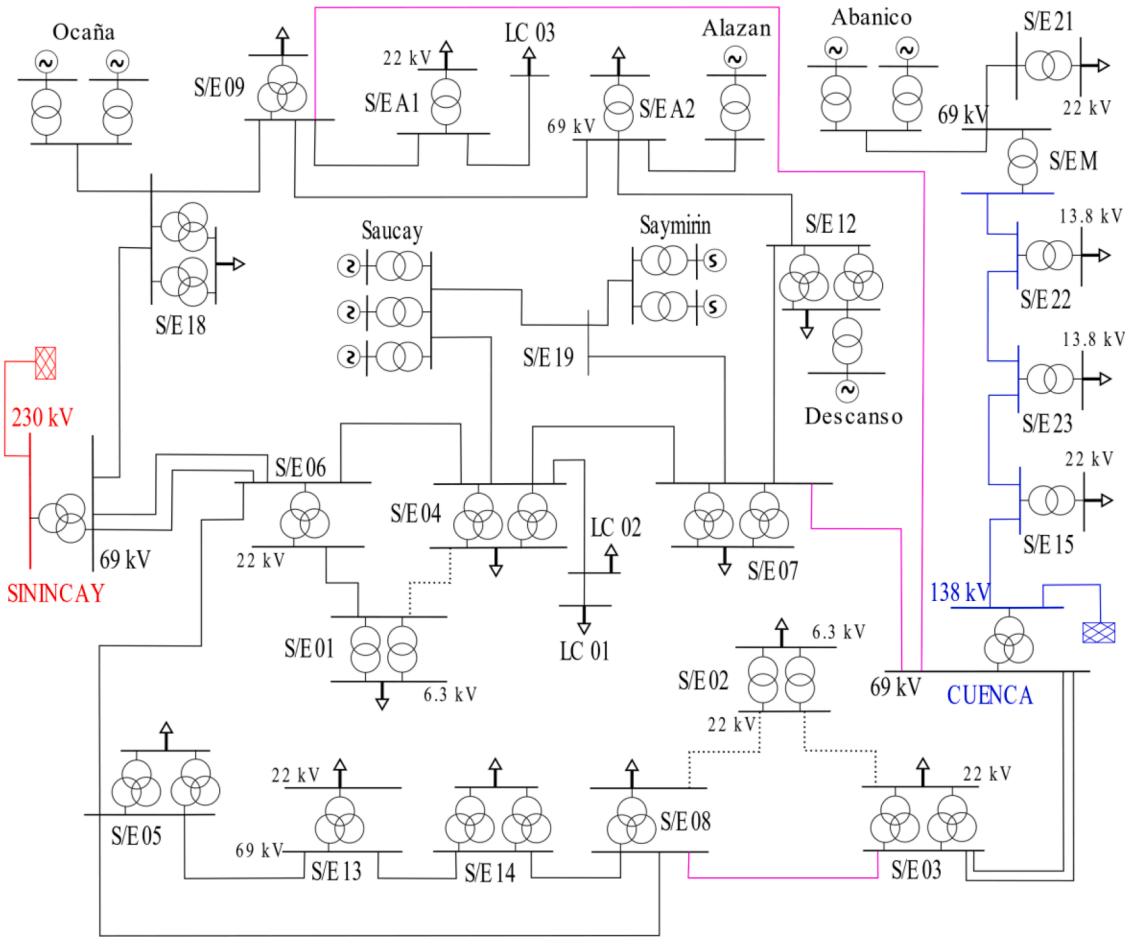

Fig. 9. Subtransmission network configuration for Solution 4.

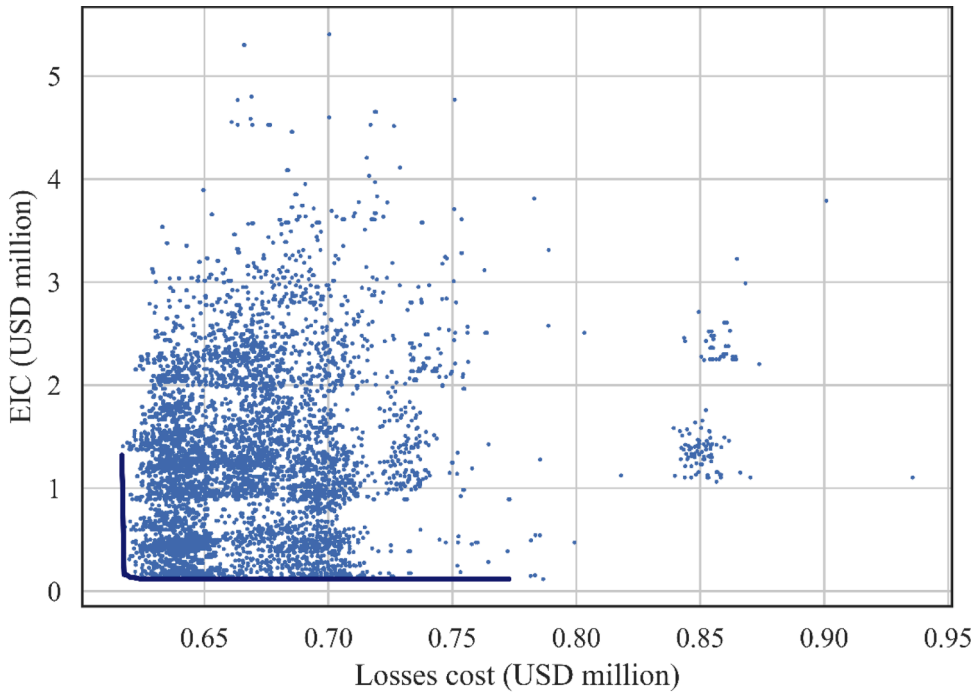

Fig. 10. Scatter plot of the feasible solutions found with brutal force with *Nsl*=4 and Pareto optimal front (blue line).

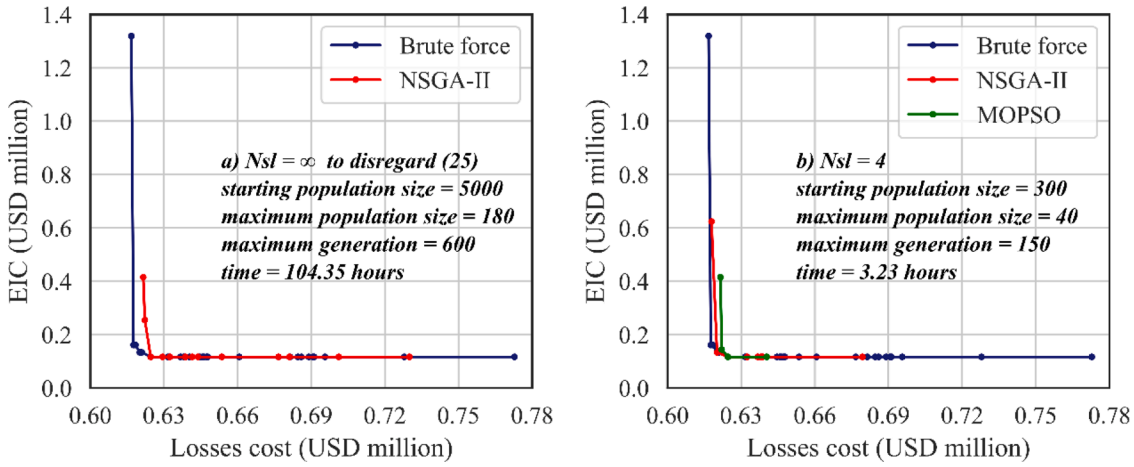

Fig. 11. Pareto fronts found using the NSGA-II algorithm and brute force.

different configurations.

As a future work, it is proposed to model the uncertainties of the generation connected to the subtransmission system, mainly from intermittent renewable sources. In the discussion of the results, a subsequent short-circuit analysis was carried out; thus, future research could incorporate restrictions due to high short-circuit currents. The importance of reliability costs for distribution systems was highlighted, so more work is needed to quantify the social effects of power outages. In turn, an integral analysis and modeling of the subtransmission and primary distribution systems is ideal, mainly to articulate the analysis of contingencies and reliability between both systems. If a new topological configuration has been established, as a result of this line switching optimization, a next phase of complementary analyzes will be necessary, such as electromagnetic transients, adjustments to tele-protection schemes, systemic protection and differential protection, among others.

Credit Author Statement

Zambrano-Asanza Sergio: Conceptualization, Methodology, Software, Validation, Formal Analysis, Investigation, Resources, Data Curation, Writing - Original Draft, Writing - Review & Editing, Visualization, Supervision, Founding Acquisition; **Proano Barros Tatiana:** Methodology, Software, Formal Analysis, Investigation, Data Curation; **Banegas Dutan Stalin:** Methodology, Software, Formal Analysis, Investigation, Data Curation; **Lema Guaman Edwin:** Methodology, Software, Validation, Formal Analysis, Investigation, Resources, Data Curation; **Franco John Fredy:** Conceptualizatio, Validation, Formal Analysis, Investigation, Writing - Original Draft, Writing - Review & Editing, Visualization, Project Administration, Founding Acquisition.

Declaration of Competing Interest

None.

Acknowledgments

The authors would like to thank “Empresa Eléctrica Regional Centro Sur C.A.”, Electric Distribution Utility of Ecuador, for the provided information and collaborative support.

This work was supported by the Brazilian institutions: Coordination for the Improvement of Higher Education Personnel (CAPES) - Finance Code 001, and the São Paulo Research Foundation (FAPESP), under grants 2015/21972-6 and 2017/02831-8.

Appendix A

Table 7 and Table 8.

Table 7
Three-winding transformers of the subtransmission system

		Rater Power [MVA]			Rated Voltage [kV]			Vector Group			Reactance X [p.u.]		
Substation	Name	HV	MV	LV	HV	MV	LV	HV	MV	LV	HV-MV	MV-LV	LV-HV
CUENCA	CUE	100	100	27	138	69	13.8	YN	YN	D	0.069	0.068	0.093
S/E 03	T034	24	24	8	69	22	13.8	YN	YN	D	0.081	0.010	0.044
S/E 03	T035	24	24	8	69	22	13.8	YN	YN	D	0.081	0.010	0.044
S/E 04	T041	24	24	8	69	22	13.8	YN	YN	D	0.081	0.010	0.044
S/E 04	T042	24	24	8	69	22	13.8	YN	YN	D	0.081	0.010	0.044
S/E 05	T051	24	24	8	69	22	13.8	YN	YN	D	0.085	0.010	0.045
S/E 05	T052	24	24	8	69	22	13.8	YN	YN	D	0.081	0.010	0.044
S/E 06	T061	10	10	3.33	69	22	4.2	YN	YN	D	0.087	0.013	0.039
S/E 07	T071	10	10	3.33	69	22	2.39	YN	YN	D	0.090	0.013	0.044
S/E 07	T072	12.5	12.5	4	69	22	6.3	YN	YN	D	0.094	0.010	0.044
S/E 08	T081	24	24	8	69	22	2.39	YN	YN	D	0.089	0.010	0.045
S/E 09	T091	10	10	3.33	69	22	2.39	YN	YN	D	0.090	0.010	0.044
S/E 12	T122	10	10	3.33	69	22	2.39	YN	YN	D	0.090	0.010	0.044
S/E 12	T123	10	10	3.33	69	22	2.39	YN	YN	D	0.090	0.014	0.039
S/E 13	T131	10	10	3.33	69	22	4.2	YN	YN	D	0.087	0.013	0.039
S/E 14	T141	10	10	3.33	69	22	4.28	YN	YN	D	0.090	0.014	0.039
S/E 14	T142	24	24	8	69	22	13.8	YN	YN	D	0.081	0.010	0.044
S/E 18	T181	10	10	3.33	69	22	4.28	YN	YN	D	0.090	0.014	0.039
S/E 18	T182	24	24	8	69	22	13.8	YN	YN	D	0.081	0.010	0.044

Table 8
Two-winding transformers of the subtransmission system

Substation	Name	Power [MVA]	Rated Voltage [kV]		Vector Group		X [p.u.]	R [p.u.]
			HV	LV	HV	LV		
Abanico	T Abanico 1	18	69	4.16	YN	D	0.102	0.006
Abanico	T Abanico 2	27	69	4.16	D	YN	0.120	0.004
Ocaña	T Ocaña 1	15	69	13.8	YN	D	0.085	0.003
Ocaña	T Ocaña 2	15	69	13.8	YN	D	0.085	0.003
S/E 01	T011	5	22	6.3	D	YN	0.059	0.004
S/E 01	T012	10	22	6.3	D	YN	0.056	0.006
S/E 02	T021	5	22	6.3	D	YN	0.059	0.004
S/E 02	T022	10	22	6.3	D	YN	0.056	0.006
Saymirin	T111	10	69	2.4	YN	D	0.090	0.009
Saymirin	T112	10	69	6.3	YN	D	0.077	0.005
Descanso	T121	20	22	6.3	YN	D	0.120	0.006
Saucay	T201	10	69	4.16	YN	D	0.090	0.009
Saucay	T202	10	69	4.16	YN	D	0.090	0.009
Saucay	T203	10	69	4.16	YN	D	0.090	0.009
S/E 15	T151	16	138	22	D	YN	0.070	0.003
S/E 21	T213	10	69	22	D	YN	0.090	0.006
S/E 21	T214	24	69	22	D	YN	0.081	0.005
S/E 22	T221	6,67	138	13.8	D	YN	0.069	0.008
S/E 23	T231	6,67	138	13.8	D	YN	0.069	0.008
Alazan	TAlazán	10	69	6.6	YN	D	0.075	0.001
S/E A1	TEEAz1	10	69	22	D	YN	0.074	0.003
S/E A2	TEEAz2	10	69	22	D	YN	0.074	0.003
S/E M	THA 138	48	138	69	YN	D	0.067	0.001

References

[1] CIGRE /CIRED WG CC 01, Interaction between transmission and distribution system planning, 1995.

[2] T. Gönen, Electric power distribution engineering, 3rd ed., CRC Press, 2014. https://www.crcpress.com/Electric-Power-Distribution-Engineering-Third-Edition/Gonen/p/book/9781482207002 (accessed April 12, 2018).

[3] M.N. Eggleton, E. Van Geert, M. Mazzoni, W.L. Kling, Network structure in sub-transmission systems features and practices in different countries, in: IEE Conf. Publ, 1993. https://ieeexplore.ieee.org/document/225814 (accessed April 21, 2021).

[4] E.B. Fisher, R.P. O'Neill, M.C. Ferris, Optimal transmission switching, IEEE Trans. Power Syst. 23 (2008) 1346–1355, https://doi.org/10.1109/TPWRS.2008.922256.

[5] K.W. Hedman, M.C. Ferris, R.P. O'Neill, E.B. Fisher, S.S. Oren, Co-optimization of generation unit commitment and transmission switching with N-1 reliability, IEEE Trans. Power Syst. 25 (2010) 1052–1063, https://doi.org/10.1109/TPWRS.2009.2037232.

[6] M. Jabarnejad, Approximate optimal transmission switching, Electr. Power Syst. Res. 161 (2018) 1–7, https://doi.org/10.1016/J.EPSR.2018.03.021.

[7] M. Flores, L.H. Macedo, R. Romero, Alternative mathematical models for the optimal transmission switching problem, IEEE Syst. J. 15 (2021) 1245–1255, https://doi.org/10.1109/JSYST.2020.3000978.

[8] M. Flores, R. Romero, J.F. Franco, An analysis of the optimal switching problem in transmission systems, in: 2017 IEEE PES Innov. Smart Grid Technol. Conf. - Lat. Am. ISGT Lat. Am, Institute of Electrical and Electronics Engineers Inc., 2017, pp. 1–5, https://doi.org/10.1109/ISGT-LA.2017.8126720, 2017.

[9] J.D. Fuller, R. Ramasra, A. Cha, Fast heuristics for transmission-line switching, IEEE Trans. Power Syst. 27 (2012) 1377–1386, https://doi.org/10.1109/TPWRS.2012.2186155.

[10] C. Liu, J. Wang, J. Ostrowski, Heuristic prescreening switchable branches in optimal transmission switching, IEEE Trans. Power Syst. 27 (2012) 2289–2290, https://doi.org/10.1109/TPWRS.2012.2193489.

[11] C. Zhang, J. Wang, Optimal transmission switching considering probabilistic reliability, IEEE Trans. Power Syst. 29 (2014) 974–975, https://doi.org/10.1109/TPWRS.2013.2287999.

[12] S. Pal, S. Sen, J. Bera, S. Sengupta, Regenerative and combinatorial random variable based particle swarm optimization towards optimal transmission switching, Appl. Soft Comput. J. 95 (2020), 106529, https://doi.org/10.1016/j.asoc.2020.106529.

[13] M.T. Hagh, M.Z. Gargari, M.J.V. Pakdel, Sequential analysis of optimal transmission switching with contingency assessment, IET Gener. Transm. Distrib. 12 (2018) 1390–1396, https://doi.org/10.1049/iet-gtd.2017.0435.

[14] J.F.L. Van Casteren, M.H.J. Bollen, M.E. Schmieg, Reliability assessment in electrical power systems: the Weibull-Markov stochastic model, IEEE Trans. Ind. Appl. 36 (2000) 911–915, https://doi.org/10.1109/28.845070.

[15] R. Billinton, W. Li, Reliability Assessment of Electric Power Systems Using Monte Carlo Methods, Springer US, 1994, https://doi.org/10.1007/978-1-4899-1346-3.

[16] A. Tabares, G. Munoz-Delgado, J.F. Franco, J.M. Arroyo, J. Contreras, An enhanced algebraic approach for the analytical reliability assessment of distribution systems, IEEE Trans. Power Syst. 34 (2019) 2870–2879, https://doi.org/10.1109/TPWRS.2019.2892507.

[17] G. Munoz-Delgado, J. Contreras, J.M. Arroyo, Reliability assessment for distribution optimization models: A non-simulation-based linear programming approach, IEEE Trans. Smart Grid. 9 (2018) 3048–3059, https://doi.org/10.1109/TSG.2016.2624898.

[18] Z. Li, W. Wu, B. Zhang, X. Tai, Analytical reliability assessment method for complex distribution networks considering post-fault network reconfiguration, IEEE Trans. Power Syst. 35 (2020) 1457–1467, https://doi.org/10.1109/TPWRS.2019.2936543.

[19] Z. Li, W. Wu, X. Tai, B. Zhang, A reliability-constrained expansion planning model for mesh distribution networks, IEEE Trans. Power Syst. 36 (2021) 948–960, https://doi.org/10.1109/TPWRS.2020.3015061.

[20] R.E. Brown, Electric Power Distribution Reliability, 2nd ed., CRC, 2002.

[21] D.P. Bernardon, V.J. Garcia, A.S.Q. Ferreira, L.N. Canha, Multicriteria distribution network reconfiguration considering subtransmission analysis, IEEE Trans. Power Deliv. 25 (2010) 2684–2691, https://doi.org/10.1109/TPWRD.2010.2041013.

[22] M.A. Tavakkoli, N. Amjady, A new AC OPF tool for sub-transmission networks considering distribution switching actions and load-transferring capability, Int. Trans. Electr. Energy Syst. 29 (2019) e12029, https://doi.org/10.1002/2050-7038.12029.

[23] K. Deb, A. Pratap, S. Agarwal, T. Meyarivan, A fast and elitist multiobjective genetic algorithm: NSGA-II, IEEE Trans. Evol. Comput. 6 (2002) 182–197, https://doi.org/10.1109/4235.996017.

[24] J.S. Nunes, A.M.L. Da Silva, J.G. De Costa, Impact of transmission and subtransmission failures on distribution reliability indices, in: 2018 Int. Conf. Probabilistic Methods Appl. to Power Syst. PMAPS 2018 - Proc, 2018, https://doi.org/10.1109/PMAPS.2018.8440306.

[25] R. Billinton, R.N. Allan, Reliability Evaluation of Power Systems, Springer US, 1996, https://doi.org/10.1007/978-1-4899-1860-4.

[26] L. Goel, R. Gupta, M.F. Ercan, Comparison of subtransmission system reliability worth for diverse systems by including health considerations, Electr. Power Syst. Res. 74 (2005) 65–72, https://doi.org/10.1016/J.EPSR.2004.10.007.

[27] S.M. Mohseni-Bonab, A. Hajebrahimi, I. Kamwa, A. Moeini, Transmission and distribution co-simulation: A review and propositions, IET Gener. Transm. Distrib. 14 (2020) 4631–4642, https://doi.org/10.1049/iet-gtd.2020.0244.

[28] DIgSILENT, DIgSILENT PowerFactory 2021, (2021) 1. https://www.digsilent.de/en/ (accessed May 8, 2021).

[29] A.T. Nguyen, S. Reiter, P. Rigo, A review on simulation-based optimization methods applied to building performance analysis, Appl. Energy. 113 (2014) 1043–1058, https://doi.org/10.1016/j.apenergy.2013.08.061.

[30] A.C. Römer, Simulation-Based Optimization, in: Simulation-Based Optim. Energy Effic. Prod., Springer Gabler, Wiesbaden, 2021, pp. 9–38, https://doi.org/10.1007/978-3-658-32971-6_2.

[31] L. Alvarado-Barrios, C. Álvarez-Arroyo, J.M. Escaño, F.M. Gonzalez-Longatt, J. L. Martinez-Ramos, Two-level optimisation and control strategy for unbalanced active distribution systems management, IEEE Access 8 (2020) 197992–198009, https://doi.org/10.1109/ACCESS.2020.3034446.

[32] J.C. Cepeda, J.L. Rueda, I. Erlich, A.W. Korai, F.M. Gonzalez-Longatt, Mean–variance mapping optimization algorithm for power system applications in DIgSILENT PowerFactory. PowerFactory Appl. Power Syst. Anal, Springer, Cham, 2014, pp. 267–295, https://doi.org/10.1007/978-3-319-12958-7_12.

[33] J. Xu, R. Yao, F. Qiu, Mitigating cascading outages in severe weather using simulation-based optimization, IEEE Trans. Power Syst. 36 (2021) 204–213, https://doi.org/10.1109/TPWRS.2020.3008428.

[34] E.G. Morquecho, S.P. Torres, C.A. Castro, An efficient hybrid metaheuristics optimization technique applied to the AC electric transmission network expansion

planning, Swarm Evol. Comput. 61 (2021), 100830, https://doi.org/10.1016/j.swevo.2020.100830.
[35] A. Konak, D.W. Coit, A.E. Smith, Multi-objective optimization using genetic algorithms: A tutorial, Reliab. Eng. Syst. Saf. 91 (2006) 992–1007, https://doi.org/10.1016/j.ress.2005.11.018.
[36] DIgSILENT GmbH, DIgSILENT PowerFactory - User Manual, 2020. Gomaringen, Germany, https://www.digsilent.de/en/powerfactory.html.
[37] B.W. Tuinema, J.L. Rueda Torres, A.I. Stefanov, F.M. Gonzalez-Longatt, M.A.M. M. van der Meijden, Probabilistic Reliability Analysis of Power Systems, 1st ed., Springer International Publishing, 2020 https://doi.org/10.1007/978-3-030-43498-4.
[38] C.D. López, J.L. Rueda Torres, Python scripting for DIgSILENT PowerFactory: Leveraging the python API for scenario manipulation and analysis of large datasets. Adv. Smart Grid Funct. Based PowerFactory, Springer Verlag, 2018, pp. 19–48, https://doi.org/10.1007/978-3-319-50532-9_2.
[39] M. Stifter, F. Andrén, R. Schwalbe, W. Tremmel, Interfacing PowerFactory: Co-simulation, real-time simulation and controller hardware-in-the-loop applications. PowerFactory Appl. Power Syst. Anal, Springer, Cham, 2014, pp. 343–366, https://doi.org/10.1007/978-3-319-12958-7_15.
[40] CIGRE, Methods to consider interruption cost in power systems analysis, 2001. Paris, France, https://e-cigre.org/publication/ELT_197_8-methods-to-consider-interruption-cost-in-power-systems-analysis (accessed June 6, 2021).
[41] R. Billinton, W. Wangdee, Approximate methods for event-based customer interruption cost evaluation, IEEE Trans. Power Syst. 20 (2005) 1103–1110, https://doi.org/10.1109/TPWRS.2005.846098.
[42] IEEE - Distribution Reliability Working Group, IEEE Guide for Electric Power Distribution Reliability Indices, IEEE Std 1366^{TM}-2012 (2012). https://standards.ieee.org/standard/1366-2012.html (accessed June 13, 2021).
[43] M.A. Ponce-Jara, M. Castro, M.R. Pelaez-Samaniego, J.L. Espinoza-Abad, E. Ruiz, Electricity sector in Ecuador: An overview of the 2007–2017 decade, Energy Policy 113 (2018) 513–522, https://doi.org/10.1016/J.ENPOL.2017.11.036.
[44] CIGRE, Transformer reliability survey, 2015, p. 122. Working-Group-A2.37.
[45] J. Kennedy, R.C. Eberhart, Discrete binary version of the particle swarm algorithm, Proc. IEEE Int. Conf. Syst. Man Cybern. 5 (1997) 4104–4108, https://doi.org/10.1109/ICSMC.1997.637339.